Phase synchronization in noise-driven bursting neurons

Xiufeng Lang,[1,*] Qishao Lu,[2] and Jürgen Kurths[3,4]
[1]*School of Chemistry and Environment, Beihang University, 100191 Beijing, China*
[2]*Department of Dynamics and Control, Beihang University, 100191 Beijing, China*
[3]*Institute of Physics, Humboldt University, 12489 Berlin, Germany*
[4]*Potsdam Institute for Climate Impact Research, 14473 Potsdam, Germany*
(Received 27 March 2010; revised manuscript received 16 June 2010; published 11 August 2010)

The generation and synchronization of bursts are studied in intrinsically spiking neurons due to stimulation with random intracellular calcium fluctuations. It is demonstrated that sufficiently strong noise could induce qualitative change in the firing patterns of a single neuron from periodic spiking to bursting modes. The dynamical mechanism of noise-induced bursting is presented based on a global bifurcation analysis. Furthermore, it is found that a pair of uncoupled and nonidentical spiking neurons, subjected to a common noise, can exhibit synchronous firing in terms of noise-induced bursting. Furthermore, the synchronization is overall enhanced with the noise intensity increasing, and synchronization transitions are exhibited at intermediate noise levels.

DOI: 10.1103/PhysRevE.82.021909 PACS number(s): 87.19.lm, 87.19.lc, 05.45.Xt, 87.10.Mn

I. INTRODUCTION

In the past decades, constructive effects of noise in nonlinear systems have been investigated extensively in the context of noise-induced transition [1] and noise-induced synchronization [2]. Noise-induced transition means that noise may lead to the appearance of new regimes which are not observed in the corresponding noise-free system. There are many theoretical and experimental studies of such phenomenon in biological systems [3–6], including noise-induced spiking or bursting in neural models. Noise-induced synchronization means that a common external noise input to two independent systems could give rise to synchronized motion of both systems. Such synchronization has been demonstrated in various systems from physics, ecology, and biology [7–11]. In particular, Kurths *et al.* reported a mechanism for noise-induced complete synchronization of chaotic systems [10], which may be used to explain an experimental finding of neural information coding that a fluctuating input rather than a constant input could greatly improve reliability of spiking time in neocortical neurons [12]. The frontier of this interest has shifted to noise-induced phase synchronization of systems with chaotic [11] or limit cycle dynamics [13,14] in recent years.

Bursting is a fundamental regime of neuronal behavior, exhibiting trains of spikes of action potential mediated by periods of silence [15]. Biophysical and dynamical mechanisms of burst generation in a single neuron or a neural network have been investigated quite scrupulously in the deterministic limit [16–19]. Meanwhile, much attention has been focused on bursting induced by noise [5,6,20,21], due to ubiquity of noise in the nervous systems [22]. For example, it has been reported that bursting could be produced in an excitable or subthreshold oscillatory regime of noisy neuron models [6,20]. Neiman *et al.* [21] observed experimentally noise-induced transition from quasiperiodically spiking to bursting in responses of Paddlefish electroreceptor afferents. Nevertheless, mechanisms underlying the noise-induced bursting (NIB) remain unclear.

Neural synchronization has been suggested as particularly relevant for neuronal signal transmission and coding. Recently, burst synchronization of neurons, referred to only the envelopes of the spikes in a population of bursting neurons, attracts more interest [23–28]. For instance, burst synchronization can be achieved readily if the neurons are coupled, as analyzed theoretically [23,24] and experimentally [26,27]. Interestingly, Neiman *et al.* [28] reported that burst synchronization could also be achieved via a mechanism of noise-induced slow dynamics in uncoupled sensory neurons with fast spiking dynamics. Characteristics of the noise-induced burst synchronization (NIBS) in uncoupled neurons are not well understood.

Here, in the context of noise-induced transition and noise-induced phase synchronization, we will investigate NIB and NIBS in a pair of uncoupled, nonidentical and conductance-based neuronal models in detail. It is found that firing patterns of these neurons undergo a qualitative change from a periodic spiking mode to a bursting mode in the presence of strong noise. A dynamical origin of such phenomenon is provided in virtue of a global bifurcation analysis of the corresponding deterministic model. In addition, noise-induced burst synchronization and synchronization transitions are demonstrated in the two uncoupled nonidentical neurons.

II. MODEL

The Plant's model for bursting nerve cells in Aplysia R-15 [29] and thermoreceptors is chosen to investigate nontrivial effects of intracellular calcium fluctuations on spiking dynamics of the neurons. In this model, the spike-generating mechanisms are of the familiar Hodgkin-Huxley type (i.e., with fast, V-dependent inward and outward currents) and the slow processes include a slow inward current and the slow changes in intracellular free calcium concentration, which activate an outward current or inactivate an inward current.

*Corresponding author; lxf125@yahoo.cn

The Plant's model is governed by the following equations,

$$C_m \frac{dV}{dt} = -g_{Na} \cdot m_\infty^3(V) \cdot h \cdot (V - V_{Na}) - g_{Ca} \cdot x \cdot (V - V_{Ca}) - (g_K \cdot n^4 + g_{K-Ca} \cdot y/(0.5 + y)) \cdot (V - V_K) - g_L \cdot (V - V_L), \quad (1)$$

$$\frac{dh}{dt} = \lambda \cdot [h_\infty(V) - h]/\tau_h(V), \quad (2)$$

$$\frac{dn}{dt} = \lambda \cdot [n_\infty(V) - n]/\tau_n(V), \quad (3)$$

$$\frac{dx}{dt} = [x_\infty(V) - x)]/\tau_x, \quad (4)$$

$$\frac{dy}{dt} = \rho \cdot [K_c \cdot x \cdot (V_{Ca} - V) - y] + \xi(t), \quad (5)$$

where V is a fast variable representing the membrane voltage; h, n, x are V-dependent, gating variables of sodium, potassium and mixed sodium and calcium, respectively; y is the intracellular free calcium concentration. Note that the calcium concentration y is dimensionless, since the free calcium concentration has been scaled by the dissociation constant for binding to a Ca^{2+} channel [30]. Herein, the parameter ρ and τ_x are equal to 0.000 15 ms^{-1} and 9400 ms, respectively. The voltage dependency of x_∞ is $x_\infty(V) = 1/[\exp\{A \cdot (B - V)\} + 1]$, where $A = 0.3$ and $B = -40$. These values are taken from the caption of Fig. 6 in Ref. [30]. A description of other parameters and nonlinear functions for Eqs. (1)–(4) can be found in Appendix I of Ref. [30]. The parameter K_c is chosen as a control the parameter here and taken as 0.0032 mV^{-1} to make the neuron periodically spiking. $\xi(t)$ is a Gaussian white noise with zero mean value $\langle \zeta(t) \rangle = 0$ and the autocorrelation function $\langle \xi(t_1)\xi(t_2) \rangle = 2D\delta(t_1 - t_2)$, in which D is the noise intensity. Because experiments reports observed fluctuations in the baseline values of calcium and variations in the amplitudes and widths of intracellular calcium oscillations [31] and theoretical works well reproduced these stochastic effects in stochastic models driven by the white noise [32], we adopt the white noise to cause fluctuations of the intracellular calcium concentration here. It should be noted that in our simulations, we set that the intracellular calcium concentration is equal to 0 when negative values are obtained from Eq. (5).

The deterministic model [i.e., Eqs. (1)–(5) without the noise term $\xi(t)$] is integrated numerically by using the Euler method with a time step of 0.01 ms. The stochastic model (1)–(5) is calculated numerically by using the Euler-Maruyama algorithm [33] with the same time step. The time evolution of the transient process is discarded in the simulation results. The values of the mean interburst intervals $\langle \tau_b \rangle$, the regularity factor R, the synchronous factor ρ_{ps} and the average synchronization epochs S_{ep} are obtained by averaging over 20 independent runs.

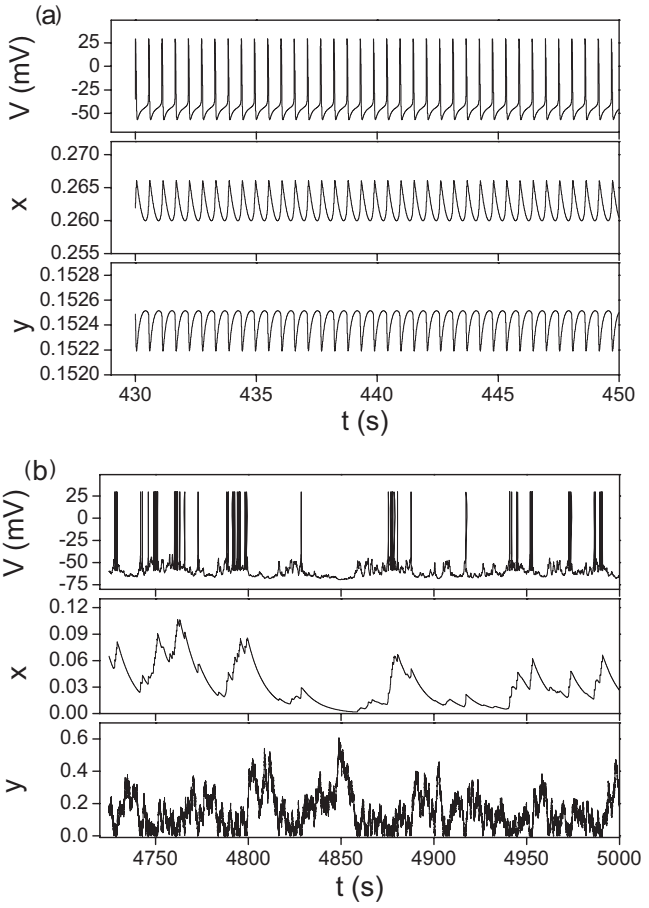

FIG. 1. Time series of the membrane voltage V, the gating variable x, and the intracellular free calcium concentration y: (a) the deterministic neuron model ($D = 0$) and (b) the noise intensity ($D = 0.003$).

III. RESULTS AND DISCUSSION

A. Noise-induced bursting in a single neuron

A simulation is implemented as follows: the single neuronal model is driven by the deterministic component only up to $t = 450$ s, by which time rhythmic spiking with the period $T = 0.547$ s is established, as shown in the top panel of Fig. 1(a). After this moment, noise with $D = 0.003$ is switched on, then the neuron produces bursts, as shown in the top panel of Fig. 1(b), and the firing patterns of the neuron changes drastically. From the middle and bottom panel in Figs. 1(a) and 1(b), it is found that as the noise intensity increases, the values of gating variable x significantly decrease and the amplitude of the calcium concentration y greatly increases, which might result in a qualitative change in the firing pattern (see Fig. 4(b), discussed below). Such a change of the firing mode in a single neuron is clearly manifested in Fig. 2, where histogram distribution of the interspike intervals (ISI) in the presence of noise is shown. When the noise intensity $D = 0.000\,005$, only a narrowband peak appears in Fig. 2(a) and the value of ISI, corresponding to the peak tip, is very close to the period T. This indicates that the spiking pattern driven by a weak noise just change quantitatively, compared with the deterministic periodic spiking

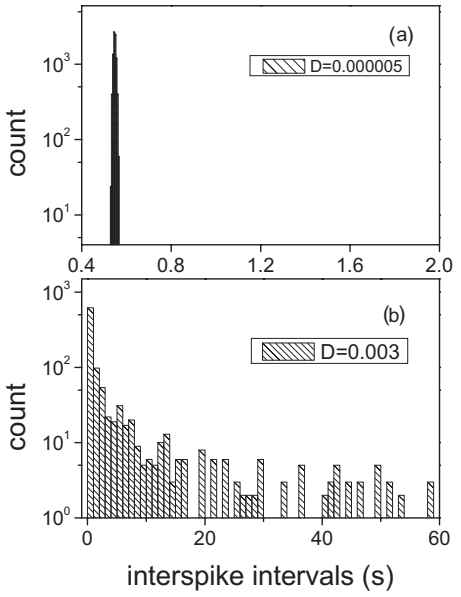

FIG. 2. Histogram distribution of interspike intervals in the model during stimulation with white noise of $D=0.000\,005$ (a) and $D=0.003$ (b).

pattern. In contrast, as $D=0.003$, a broadband distribution is generated in Fig. 2(b) and the values of ISI span a long range of time, which implies that slow clusters of spiking and fast spiking inside each cluster coexist in the firing train for stronger noise, characterizing a bursting dynamics.

NIB can be described by plotting the mean interburst interval $\langle \tau_b \rangle$ as a function of the noise intensity D [see Fig. 3(a)]. In the figure, $\langle \tau_b \rangle$ presents a U-shape change and its minimum is much larger than the deterministic period T. This illustrates that NIB involves a new characteristic slow time scale, manifested in quiescent epochs between the bursts. The phenomenon is also confirmed for the parameter $K_c=0.0034$, as shown in Fig. 3(a). Such change of $\langle \tau_b \rangle$ in the Plant's model might be attributed to the interplay between the noise and the intrinsic dynamics of the models. In addition, we study the regularity of the bursts in the noise-induced firing patterns. It is characterized as follows: $R = \frac{\sqrt{Var(\tau_b)}}{\langle \tau_b \rangle}$, where smaller values of R imply better regularity. As shown in Fig. 3(b), R decreases monotonously with increasing D, demonstrating that the regularity of the noise-induced bursts is enhanced when the noise intensity increases. Note that there is no minimum for intermediate values of D in contrast to Fig. 3(a).

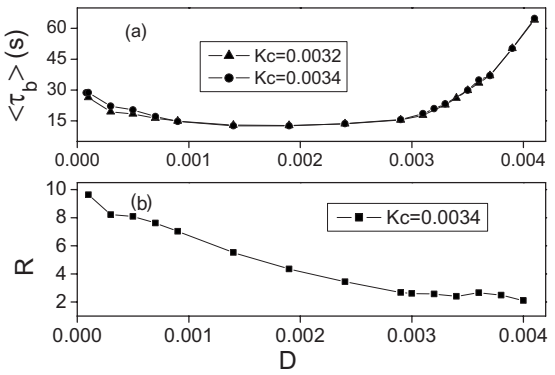

FIG. 3. (a) Mean interburst interval $\langle \tau_b \rangle$ versus the noise intensity D; (b) Regularity factor R as a function of D.

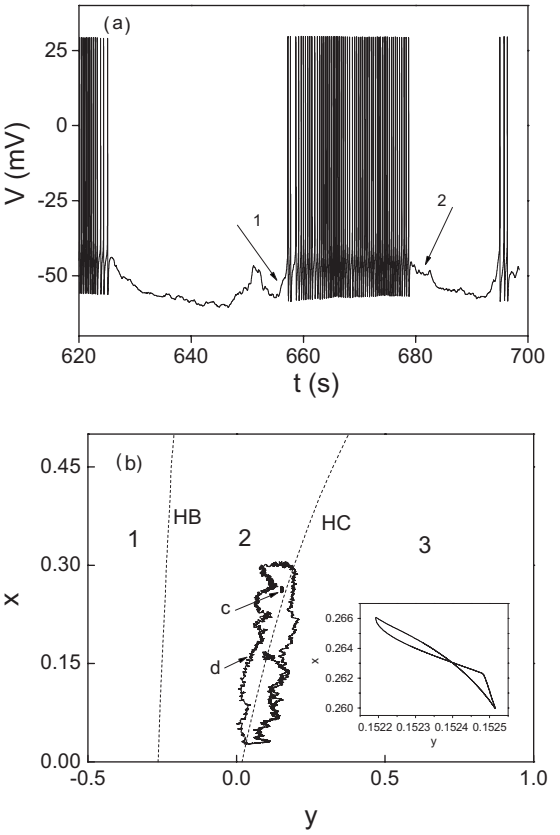

FIG. 4. (a) Time series of the membrane voltage V at $D=0.0006$; (b) Projection from HB and HC curves in the fast subsystem of the Plant's model onto the y-x plane. Regimes 1, 2, and 3 correspond to the steady state, periodic spiking state, and steady state of V in the fast subsystem, respectively. The inset shows the enlargement of orbit c, corresponding to the periodic spiking response of V. Orbit d is a stochastic cycle which drives V to generate the bursting response.

To explain the dynamic origin of NIB, we analyze the bifurcations of the dynamics of bursting in the deterministic Plant's model first. The dynamics of the bursting has been dissected with a fast/slow dynamics analysis by Rinzel *et al.* [32]. The process was carried out as follows. At first, the whole system is divided into a fast subsystem [i.e., Eqs. (1)–(3)] and a slow one [i.e., Eqs. (4) and (5)], and then the dynamics of the fast subsystem is studied when fixing x and taking y of the slow subsystem as a control parameter. It is found that V of the fast subsystem undergoes a Hopf bifurcation (HB) and a Homoclinic bifurcation (HC) with y increasing. A projection from the HB and HC curves onto the y-x plane is shown in Fig. 4(b). According to the aforementioned bifurcation analysis of the fast subsystem, the membrane voltage V stays in stable steady states in region 1 to the left side of the HB curve and in region 3 to the right side of the HC curve, and lies in a periodic spiking state in region 2 between the curves.

As illustrated by the orbit c in Fig. 4(b), weak oscillations of the slow variables x and y just stay in region 2 (see its

enlargement in the inset), which yields the repetitively spiking of the fast variables V in Fig. 1(a). When adding noise with the intensity $D=0.0006$, the amplitudes of some stochastic cycles are strongly amplified and these cycles typically cross the HC curves, as exemplified by the orbit d in Fig. 4(b). Such stochastic oscillations produce the bursting patterns in Fig. 4(a). The generation of bursting could be interpreted as follows: when the slow variable y passes the HC curve from region 3 and enters into region 2, the fast variable V could make a change from the steady state to the spiking state [see arrow 1 in Fig. 4(a)], switching on an active phase of a burst. When the variable y crosses the HC curve from region 2 and enters into region 3, the variable V would terminate the spiking state and recovers the rest state [see arrow 2 in Fig. 4(a)], turning on a silent phase of a burst. Repetition of this process leads to the bursting patterns of a neuron.

From a biophysical point of view, the noise-induced bursts might be understood as follows. The occurrence of positive fluctuations in the noise input improves accumulation of the intracellular calcium during the repetitively spiking, which turns on a Ca-activated, potassium channel with conductance $g_{K\text{-}Ca}$, yielding an outward current. The current counteracts the slow inward current and eventually terminates the spiking state. During the rest state, the occurrence of negative fluctuations in the noise input accelerates removal of the intracellular calcium, decreasing the outward current. The consequent slow depolarization eventually leads to reactivation of the slow V-dependent inward current, and thus to an activation of the rapid, spike-generating currents.

Dynamical and biophysical interpretations of the noise-induced bursting in the Plant's neuronal model might be helpful to understand experimental findings of noise-induced bursting in the sensory neurons [21,28]. In addition, Longtin [20] has also reported a noise-induced bursting pattern in the Plant's model. In contrast to our work, he choose the different deterministic dynamics and noise source in the investigation of NIB, which lead to a different generation mechanism for the noise-induced bursting in his work from that described in our work. For example, he adopted a deterministic model with slow waves but no spikes, and studied the effects of the membrane voltage fluctuations on the spiking patterns. In the present work, the deterministic model stays in a periodic spiking state and the effects of the intracellular calcium fluctuations on the spiking patterns are investigated. Due to these differences, it is reasonable to conclude that the membrane voltage fluctuations induce fast spiking on the slow waves to produce the bursting pattern in Longtin's work, while the calcium concentration fluctuations produces slow bursting on the fast and repetitive spiking to yield the bursting pattern in our work.

B. Noise-induced burst synchronization in nonidentical neurons

Due to the fact that neurons in an array typically have widely distributed natural frequencies and include statistically independent internal noise, synchronization with weaker degree, i.e., phase synchronization (PS), has been studied in nonidentical neurons [7,11,34,35]. Motivated by a recent experiment of the noise-induced burst synchronization in electroreceptor afferents [28], we investigate burst synchronization of two uncoupled and nonidentical spiking neurons stimulated by a common noise in the context of noise-induced phase synchronization.

To characterize the coincidence of bursts in both neurons, we define a phase variable for the variable V as [34],

$$\varphi(t) = 2\pi\left(k + \frac{(t-\tau_k)}{(\tau_{k+1}-\tau_k)}\right), \tag{6}$$

where $\tau_k < t < \tau_{k+1}$, and τ_k is the firing time at which the kth burst starts, detected in numerical simulations when the membrane potential V exceeds a threshold value of 0 mV and ISI is larger than a critical value of 3000 ms. It should be noted that the ISI criteria used to identify the bursts is chosen on the basis of the ISI histogram distribution [see Fig. 2(b)]. The most common approach to study PS in stochastic systems is to compute the probability of the distribution of the cyclic phase difference $P(\Delta_c\varphi)$ on $[-\pi,\pi]$, where $\Delta_c\varphi = \Delta\varphi \bmod(2\pi)$. PS is then interpreted in a statistical sense [34]: peaks of $P(\Delta_c\varphi)$ manifest preferred phase differences and the corresponding peak's sharpness characterizes the degree of stochastic phase locking. Phase synchronization in biological and ecological systems were demonstrated by means of such statistical interpretation in recent years [36,37].

To quantify the degree of PS, we introduce the entropy of the distribution of the cyclic phase differences as follows [34]:

$$H = -\sum_{i=1}^{M} P_i \ln P_i, \tag{7}$$

where M is the number of bins and P_i is the probability that the cyclic phase difference $\Delta_c\varphi$ is in the ith bin. Normalizing H in [0, 1] by the maximal entropy $H_m=\ln M$ of the uniform distribution, the synchronization index is calculated as

$$\rho_{ps} = (H_m - H)/H_m, \tag{8}$$

where $\rho_{ps}=0$ corresponds to a uniform distribution (no synchronization) and $\rho_{ps}=1$ represents a Dirac-like distribution (perfect phase synchronization).

Both neurons driven by a common noise are described by Eqs. (1)–(5), except that the parameter K_c is different for two neurons, that is, we take $K_{c1}=0.0032$ mV^{-1} for one neuron and $K_{c2}=0.0034$ mV^{-1} for the other, which make both neurons periodically oscillate with different periods 0.547 and 1.02 s, respectively. Figure 5 shows the probability density of the cyclic phase differences in both neurons for $D=0.00008$ and 0.0025, respectively. An almost uniform distribution of the phase differences in Fig. 5(a) indicates that the neurons could not be stochastically locked in the presence of weak noise. In contrast, stronger noise produces a sharp and high peak in the probability density of Fig. 5(b), demonstrating phase locking in the neurons. Actually, such synchronization is also manifested by the mean interburst intervals in Fig. 3(a). The discrepancies in the mean interburst intervals at a low noise level shows that the average

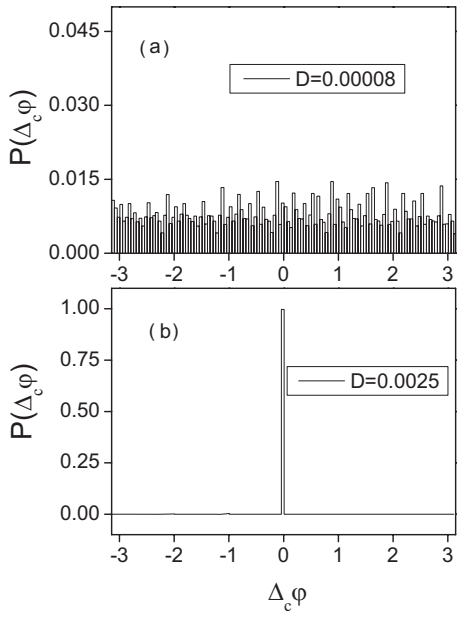

FIG. 5. Probability density of cyclic phase differences between two nonidentical and independent neurons for $D=0.000\ 08$ (a) and $D=0.0025$ (b).

frequencies of bursts in the neurons are different, while the overlap of the interburst intervals at a high noise level indicates that the average frequencies of the two neurons are the same. These results imply that the nonidentical neurons could share similar slow dynamics in the presence of sufficiently strong noise. Therefore, it is possible that a sufficient common noise could induce bursts in nonidentical and uncoupled neurons and lead to an entrainment of the slow dynamics in both neurons, producing phase synchronization.

Figure 6(a) plots the dependence of the synchronization index ρ_{ps} on the noise intensity D. It is obviously visible that overall, ρ_{ps} increases with D, demonstrating that phase synchronization appears and the synchronization degree is improved when the noise intensity increases. Surprisingly, ρ_{ps} does not smoothly increase in Fig. 6 and there exist some valleys at intermediate noise levels, which might characterize synchronization transitions induced by strong noise. Note that similar plots of ρ_{ps} versus D are obtained for 30 independent realizations and multiple minima of ρ_{ps} are also demonstrated for $K_{c1}=0.0024\ \mathrm{mV}^{-1}$ (the data are not shown here). Figure 6(b) shows the dependence of the synchronization index ρ_{ps} on the parameter K_{c1} with $K_{c2}=0.0034\ \mathrm{mV}^{-1}$ to study effects of the parameter mismatch on phase synchronization. It is obviously seen from the figure that ρ_{ps} increases monotonously as K_{c1} increases both for $D=0.0025$ and $D=0.0031$. This demonstrates that the degree of phase synchronization is enhanced when the parameter mismatch decreases. Furthermore, it is found from Fig. 6(b) that the values of ρ_{ps} for $D=0.0025$ are larger than those for $D=0.0031$ in a certain range of K_{c1}, which implies that synchronization transitions between both neurons do exist for some values of parameter mismatch in two neurons.

Synchronization fluctuations at the high noise level in Fig. 6(a) is different from the previous results that when two uncoupled neurons are subject to a common noise, the synchronization degree of noise-induced spiking (or bursting) in two neurons increases monotonously with the noise intensity [11,28]. To further explore the aforementioned phenomenon of synchronization fluctuations, we plot the phase differences of firing trains of two neurons in Fig. 7 for $D=0.0025$, 0.003, and 0.0035, respectively. As shown in Fig. 7(a), the phase differences slightly fluctuate around the value of 0, but also exhibits two outbreaks, which indicate that the phases in both neurons usually are very close, called "almost perfect PS." When D increases up to 0.003, there exist epochs of phase locking interrupted by many phase jumps in Fig. 7(b), which is the characteristic of the imperfect PS [7]. As D increases up to 0.0035, the phase differences in Fig. 7(c) fluctuate around the value 0 again and show one outbreak, demonstrating recurrence to the almost perfect PS. Noted that as the noise intensity increases up to 0.004 and 0.0041, the phase differences of firing trains in two neurons just slightly fluctuate around a constant value and do not exhibit outbreaks or phase jumps, illustrating perfect PS (data are not shown here).

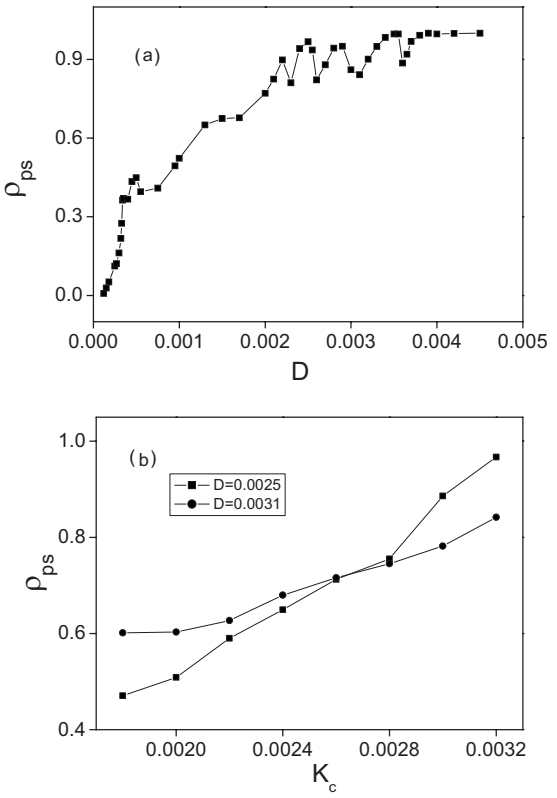

FIG. 6. (a) Dependence of phase synchronization index ρ_{ps} on the noise intensity D for $K_{c1}=0.0032\ \mathrm{mV}^{-1}$; (b) ρ_{ps} as a function of K_{c1} for $D=0.0025$ and $D=0.0031$. Herein, K_{c2} is always fixed to $0.0034\ \mathrm{mV}^{-1}$.

Moreover, we compute the average synchronization epochs S_{ep}, that is, the average time interval between two successive phase jumps, to quantify the qualitative difference in the dynamics of phase separation during the synchronization regime [7]. The dependence of S_{ep} on D is depicted in Fig. 8 to illustrate that there exist some valleys for an intermediate noise level, which is consistent with the phenomenon in Fig. 6. The nonmonotonous increasing of both ρ_{ps} and S_{ep} at in-

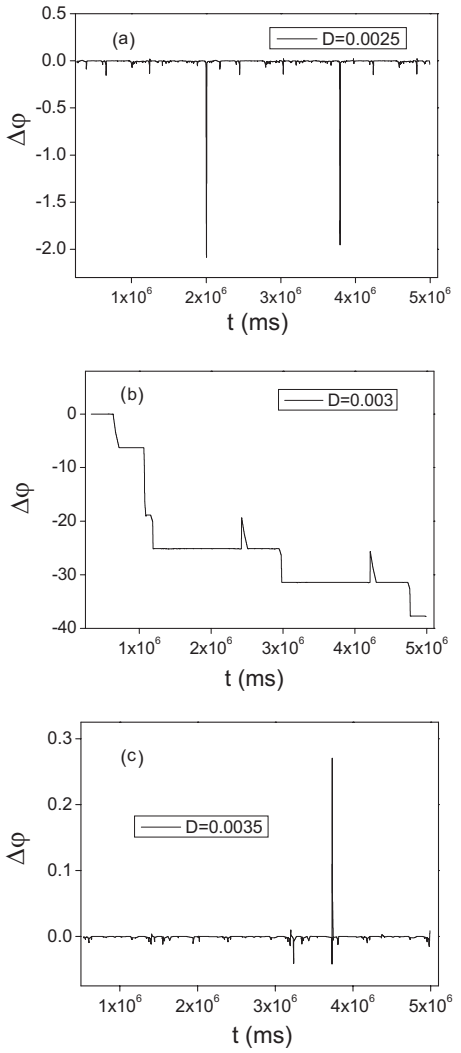

FIG. 7. Phase differences at noise intensity $D=0.0025$ (a), 0.003 (b), and 0.0035 (c).

termediate noise levels imply that as the noise intensity increases, two neurons undergo repetitive synchronization transitions between almost perfect PS and imperfect PS, and then reach perfect PS finally.

Here, we have provided a rather heuristic understanding of the synchronization transitions, but the mathematical mechanism is still an open task for future work and out of the scope of this paper. The synchronization transitions in Figs. 6(a) and 8 might be attributed to a complicated interplay between the noise and the parameter mismatch on the bursting generation in two neurons. When the noise is very low, more bursts could be produced by larger K_c due to the parameter mismatch and the time of burst occurrence in two neurons are different, leading to a weak synchronization. As the noise intensity increases, the difference of the number of bursts for different parameter K_c greatly decreases to zero, but the mean interburst intervals in both neurons just slightly decrease [see Fig. 3(a)], resulting in an enhancement of the synchronization strength and producing nearly perfect phase synchronization. However, when the noise is high, both mean interburst intervals significantly increase [see Fig. 3(a)]. According to the mechanism of burst generation, the

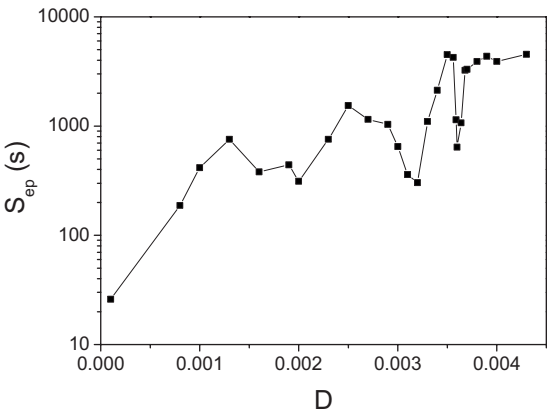

FIG. 8. Average synchronization epochs S_{ep} as a function of noise intensity D.

mean interburst intervals is influenced by the mismatch parameter and its rapid increase might amplify this influence, resulting in the differences of time of the burst occurrence in two firing patterns. This reduces the synchronization strength and causes imperfect phase synchronization. Finally, when the noise is very high, noise dominates the mean interburst intervals in two neurons over the parameter mismatch again, producing perfect phase synchronization.

IV. SUMMARY

In this paper we investigated the nontrivial effects of noise in the Plant's neuronal model, including noise-induced bursting and burst synchronization. It has been found that noise could trigger a transition in the firing pattern of single neuron from a periodic spiking mode to a bursting one. A dynamical mechanism for such bursting is provided on the basis of a global bifurcation analysis in the corresponding deterministic model. It has been demonstrated that two nonidentical and uncoupled spiking neurons, subject to a common noise, could be synchronized by means of noise-induced bursting. Furthermore, as the noise intensity increases, the synchronization degree is consistently enhanced. Interestingly, with the noise intensity increasing, both neurons undergo synchronization transitions between almost perfect and imperfect phase synchronization and finally achieve prefect phase synchronization, which is robust to the parameter mismatch in two neurons. In addition, the dependence of phase synchronization on the parameter mismatch of two neurons is also investigated.

Comparing with previous studies about deterministic bursting [16–19] and noise-induced spiking synchronization [10,11], our findings might yield some new insights into characteristics and origins of bursting and synchronization transitions in nonlinear systems driven by noise. In addition, since it is well established that fluctuations in intracellular calcium concentration are ubiquitous in cells [30], it is

expected that our results might be helpful to understand its role in synchronous bursting oscillations of a population of sensory neurons, which may be a neural mechanism for coincidence detection, and may substantially simplify the neural operations.

ACKNOWLEDGMENTS

This work was supported by the National Natural Science Foundation of China (Grant No. 10872014) and China Postdoctoral Science Foundation (Grant No. 230210143).

[1] W. Horsthemke and R. Lefever, *Noise-Induced Transitions: Theory and Applications in Physics, Chemistry, and Biology* (Springer-Verlag, Berlin, 1984).
[2] R. Toral, C. R. Mirasso, E. Hernández-García, and O. Piro, Chaos **11**, 665 (2001).
[3] A. Longtin and K. Hinzer, Neural Comput. **8**, 215 (1996).
[4] S. Tanabe and K. Pakdaman, Biol. Cybern. **85**, 269 (2001).
[5] J. Jo, H. Kang, M. Y. Choi, and D. Koh, Biophys. J. **89**, 1534 (2005).
[6] Z. Yang, Q. Lu, H. Gu, and W. Ren, Int. J. Bifurcat. Chaos **14**, 4143 (2004).
[7] S. Boccaletti, J. Kurths, G. Osipov, D. L. Valladares, and C. S. Zhou, Phys. Rep. **366**, 1 (2002).
[8] T. Zhou, L. Chen, and K. Aihara, Phys. Rev. Lett. **95**, 178103 (2005).
[9] R. F. Galán, N. Fourcaud-Trocmé, G. B. Ermentrout, and N. N. Urban, J. Neurosci. **26**, 3646 (2006).
[10] C. Zhou and J. Kurths, Phys. Rev. Lett. **88**, 230602 (2002).
[11] C. Zhou and J. Kurths, Chaos **13**, 401 (2003).
[12] Z. F. Mainen and T. J. Sejnowski, Science **268**, 1503 (1995).
[13] J. N. Teramae and D. Tanaka, Phys. Rev. Lett. **93**, 204103 (2004).
[14] H. Nakao, K. Arai, and Y. Kawamura, Phys. Rev. Lett. **98**, 184101 (2007).
[15] R. Krahe and F. Gabbiani, Nat. Rev. Neurosci. **5**, 13 (2004); S. M. Sherman, Trends Neurosci. **24**, 122 (2001); J. E. Lisman, *ibid.* **20**, 38 (1997).
[16] S. Coombes and P. C. Bressloff, *Bursting: The Genesis of Rhythm in the Nervous System* (World Scientific Publishing Co. Pte. Ltd., Singapore, 2005).
[17] E. M. Izhikevich, *Dynamical Systems in Neuroscience: The Geometry of Excitability and Bursting* (MIT Press, Cambridge, MA, 2006).
[18] P. Channell, G. Cymbalyuk, and A. Shilnikov, Phys. Rev. Lett. **98**, 134101 (2007).
[19] M. V. Ivanchenko, G. V. Osipov, V. D. Shalfeev, and J. Kurths, Phys. Rev. Lett. **98**, 108101 (2007).
[20] A. Longtin, Phys. Rev. E **55**, 868 (1997).
[21] A. B. Neiman, T. A. Yakusheva, and D. F. Russell, J. Neurophysiol. **98**, 2795 (2007).
[22] A. A. Faisal, L. P. J. Selen, and D. M. Wolpert, Nat. Rev. Neurosci. **9**, 292 (2008).
[23] M. Dhamala, V. K. Jirsa, and M. Z. Ding, Phys. Rev. Lett. **92**, 028101 (2004).
[24] M. V. Ivanchenko, G. V. Osipov, V. D. Shalfeev, and J. Kurths, Phys. Rev. Lett. **93**, 134101 (2004).
[25] Q. Y. Wang, Z. S. Duan, Z. S. Feng, G. R. Chen, and Q. S. Lu, Physica A **387**, 4404 (2008).
[26] R. C. Elson, A. I. Selverston, R. Huerta, N. F. Rulkov, M. I. Rabinovich, and H. D. I. Abarbanel, Phys. Rev. Lett. **81**, 5692 (1998).
[27] R. Segev, Y. Shapira, M. Benveniste, and E. Ben-Jacob, Phys. Rev. E **64**, 011920 (2001).
[28] A. B. Neiman and D. F. Russell, Phys. Rev. Lett. **88**, 138103 (2002).
[29] R. E. Plant, J. Math. Biol. **11**, 15 (1981).
[30] J. Rinzel and Y. S. Lee, J. Math. Biol. **25**, 653 (1987).
[31] T. Tordjmann, B. Berthon, E. Jacquemin, C. Clair, N. Stelly, G. Guillon, M. Claret, and L. Combettes, EMBO J. **17**, 4695 (1998); I. Marrero, A. Sanchez-Bueno, P. H. Cobbold, and C. J. Dixon, Biochem. J. **275**, 277 (1994).
[32] X. F. Lang and Qianshu Li, J. Chem. Phys. **128**, 205102 (2008); H. Li, Z. Hou, and H. Xin, Phys. Rev. E **71**, 061916 (2005); M. Perc and M. Marhl, Physica A **332**, 123 (2004).
[33] D. J. Higham, SIAM Rev. **43**, 525 (2001).
[34] A. Pikovsky, M. Rosenblum, and J. Kurths, *Synchronization—A Unified Approach to Nonlinear Science* (Cambridge University Press, Cambridge, England, 2001).
[35] X. F. Lang, Q. S. Lu, and L. Ji, Int. J. Mod. Phys. B (to be published).
[36] C. Schäfer, M. G. Rosenblum, J. Kurths, and H.-H. Abel, Nature (London) **392**, 239 (1998); P. Van Leeuwen, D. Geue, M. Thiel, D. Cysarz, S. Lange, M. C. Romano, N. Wessel, J. Kurths, and D. H. Grönemeyer, Proc. Natl. Acad. Sci. U.S.A. **106**, 13661 (2009).
[37] B. Blasius, A. Huppert, and L. Stone, Nature (London) **399**, 354 (1999).